

# NUMERICAL ANALYSIS OF ACOUSTIC WAVE GENERATION IN ANISOTROPIC PIEZOELECTRIC MATERIALS

Erasmus LANGER, Siegfried SELBERHERR (1)  
Peter A. MARKOWICH (2)  
Christian A. RINGHOFER (3)

- (1) Department of Physical Electronics, Technical University of Vienna / AUSTRIA  
(2) Department of Applied Mathematics, Technical University of Vienna / AUSTRIA  
(3) Mathematics Research Center, University of Wisconsin-Madison

## Abstract

We present an "Ab Initio" transient analysis of acoustic wave generation in piezoelectric materials which takes account of second order effects. The computer program we have developed for that purpose solves the fundamental differential equations in two space dimensions with the corresponding mechanical displacements and the electrical potential as dependent variables by a semi-implicit finite difference scheme rather than by wave approximations. This has become possible with acceptable usage of computer resources only by introducing a novel form of boundary conditions for the quasi infinite sagittal plane to avoid reflection phenomena. We present numerical results for  $YZ\text{-LiNbO}_3$  and ST-Cut of Quartz.

## 1. Introduction

With the increasingly widespread use of surface acoustic wave (SAW) devices, particularly filters, modeling of wave propagation phenomena in anisotropic piezoelectric materials has become eminently important. However, almost all modeling activities have been concentrated on the simulation of the extrinsic device behaviour. We present an "Ab Initio" analysis - not a simple simulation - of wave effects without neglecting second order effects, like bulk wave generation, diffraction, interaction of surface waves and bulk waves. For that purpose we have developed a computer program for the solution of the fundamental partial differential equations which describe wave propagation in arbitrary, anisotropic piezoelectric media.

There are many publications dealing with surface acoustic wave propagation but either the authors a priori postulate a wave approximation [5,6] or simulate an infinite periodic structure [3]. Our method is different since we do not anticipate the solution in any

way. We solve the fundamental equations in two space dimensions - in the sagittal plane - by a semi-implicit time integration scheme using a novel form of boundary conditions for the quasi infinite domain. Therefore, we can correctly analyze the excitation of surface and bulk waves by just considering a relatively small area below the electrodes of the transducer. The input data for our program are the geometry of the transducer fingers, the substrate material and the Euler's angles of the crystal cut. The structure and the actual values of the material dependent tensors are stored in a database for most of the common materials. However, the analysis of new materials is merely a matter of specifying the tensor data. One major objective of our investigation is the quest for physical insight into SAW devices to enable the development of simple analytic formulas for device characterization and design. The power of our analysis method lies in the general applicability with respect to the different materials and crystal cuts and the not neglected interaction between surface and bulk waves. For that reason our computer program can be used for instance to optimize a crystal cut by minimizing the acoustic power radiation in the bulk. Because of the chosen solution method the program could be extended to include non linearity effects. In this paper the transient behaviour of a transducer structure with four fingers is demonstrated for two different materials.

## 2. The Physical Model

The physical model is based on the fundamental set of equations describing acoustic wave propagation in an arbitrary piezoelectric material consisting of equations of motion (1), the linear, strain-mechanical displacement relations (2), Maxwell's equations under the quasi-static assumptions (3,4) and the linear piezoelectric constitutive relations (5,6) [1]. It is to be noted

that standard tensor notation as well as Einstein's summation convention is used.

$$\partial T_{ij} / \partial x_i = \rho \partial^2 u_j / \partial t^2 \quad (1)$$

$$S_{kl} = (\partial u_k / \partial x_l + \partial u_l / \partial x_k) / 2 \quad (2)$$

$$\partial D_i / \partial x_i = 0 \quad (3)$$

$$E_i = -\partial \varphi / \partial x_i \quad (4)$$

$$T_{ij} = c_{ijkl} \cdot S_{kl} - e_{nij} \cdot E_n \quad (5)$$

$$D_m = \epsilon_{mkl} \cdot S_{kl} + \epsilon_{mn} \cdot E_n \quad (6)$$

T denotes the stress,  $\rho$  the mass density, u the mechanical displacement, S the strain, D the electric displacement, E the electric field,  $\varphi$  the electric potential. The fourth rank tensor c is the elastic stiffness tensor, the third rank tensor e the piezoelectric tensor, and the second rank tensor  $\epsilon$  the dielectric tensor in the actual i.e. rotated coordinate system. These three tensors are the result (7,8,9) of a transformation of the unrotated quantities  $c^0$ ,  $e^0$ , and  $\epsilon^0$  according to Euler's transformation matrix V.

$$c_{ijkl} = V_{ir} \cdot V_{js} \cdot V_{kt} \cdot V_{lq} \cdot c^0_{rstq} \quad (7)$$

$$e_{ijk} = V_{ir} \cdot V_{js} \cdot V_{kt} \cdot e^0_{rst} \quad (8)$$

$$\epsilon_{ij} = V_{ir} \cdot V_{js} \cdot \epsilon^0_{rs} \quad (9)$$

By substituting (2) and (4) into equations (5) and (6) and then eliminating the mechanical stress T and the electric displacement D one obtains a system of partial differential equations in three space dimensions (j=1,2,3) which consists of three mechanical wave equations (10) and Poisson's equation (11).

$$c_{ijkl} \cdot \partial^2 u_k / \partial x_l \partial x_i - e_{kij} \cdot \partial^2 \varphi / \partial x_k \partial x_i = \rho \cdot \partial^2 u_j / \partial t^2 \quad (10)$$

$$e_{ikl} \cdot \partial^2 u_k / \partial x_l \partial x_i - \epsilon_{ik} \cdot \partial^2 \varphi / \partial x_k \partial x_i = 0 \quad (11)$$

The surface boundary conditions for the mechanical quantities result from the fact that the force component perpendicular to the surface plane vanishes, i.e.  $T_{3j} = 0$  (j=1,2,3). For Poisson's equation the surface boundary condition is derived from the fact that the electrical displacement  $D_3$  vanishes.

Now we reduce the system to the two space dimensions  $x=x_1$  and  $z=x_3$  and we define the solution vector s with its components u (mechanical displacement in x-direction), w (mechanical displacement in z-direction), and  $\varphi$  (electrical potential). This procedure leads to the

following set of equations and the surface boundary condition:

$$\mathcal{Q} \cdot s_{tt} = A \cdot s_{xx} + B \cdot s_{xz} + C \cdot s_{zz}, \quad t > 0, x \in R, z < 0 \quad (13)$$

$$D \cdot s_x + E \cdot s_z = 0 \quad (14)$$

A, B, C, D, E are 3x3 matrices and A, B, C, E are symmetric.  $\mathcal{Q}$  is a diagonal matrix whose main diagonal has the entries  $\rho, \rho, 0$ . The boundary condition (14) holds for the u,w-equations for all  $x \in R$  and for the third ( $\varphi$ ) equation on the free surface and  $\varphi = V_i(t)$  on the i-th finger.

### 3. The Numerical Algorithm

The equations for the mechanical displacements (i.e. the first two equations of (13)) can be classified as hyperbolic, the last equation (i.e. the equation for the electric potential) is elliptic, therefore (13) is a coupled hyperbolic-elliptic system of (three) differential equations.

We employ the following discretization:

$$\begin{aligned} \rho/k^2 \cdot \begin{bmatrix} u_{ij}^{n+1} - 2u_{ij}^n + u_{ij}^{n-1} \\ w_{ij}^{n+1} - 2w_{ij}^n + w_{ij}^{n-1} \\ 0 \end{bmatrix} = \\ = A/h^2 \cdot \begin{bmatrix} u_{i+1j}^n - 2u_{ij}^n + u_{i-1j}^n \\ w_{i+1j}^n - 2w_{ij}^n + w_{i-1j}^n \\ \varphi_{i+1j}^{n+1} - 2\varphi_{ij}^{n+1} + \varphi_{i-1j}^{n+1} \end{bmatrix} + \\ + B/4h^2 \cdot \begin{bmatrix} u_{i+1j+1}^n - u_{i-1j+1}^n - u_{i+1j-1}^n + u_{i-1j-1}^n \\ w_{i+1j+1}^n - w_{i-1j+1}^n - w_{i+1j-1}^n + w_{i-1j-1}^n \\ \varphi_{i+1j+1}^{n+1} - \varphi_{i-1j+1}^{n+1} - \varphi_{i+1j-1}^{n+1} + \varphi_{i-1j-1}^{n+1} \end{bmatrix} \\ + C/h^2 \cdot \begin{bmatrix} u_{ij+1}^n - 2u_{ij}^n + u_{ij-1}^n \\ w_{ij+1}^n - 2w_{ij}^n + w_{ij-1}^n \\ \varphi_{ij+1}^{n+1} - 2\varphi_{ij}^{n+1} + \varphi_{ij-1}^{n+1} \end{bmatrix} \quad (15) \end{aligned}$$

for  $i=0, \pm 1, \pm 2, \dots$ ,  $j=-1, -2, \dots$ , and  $n=1, 2, 3, \dots$ . We denoted  $h = \Delta x = \Delta z$  and  $k = \Delta t$ .  $u_{ij}^n, w_{ij}^n, \varphi_{ij}^n$  are approximations to  $u(x=ih, z=jh, t=nk)$ ,  $w(x=ih, z=jh, t=nk)$  and  $\varphi(x=ih, z=jh, t=nk)$  respectively. The initial conditions are  $u_{ij} = w_{ij} = \varphi_{ij} = 0$ .

The Neumann boundary conditions (14) are discretized fully implicitly, that means at the (n+1)-time level, and discrete Dirichlet boundary data for  $\psi_{i0}^n$  are imposed at the fingers. We remark that also the potential equation is fully implicit in (13).

Fourier analysis as described in reference [7] shows that this difference scheme is stable (that means solutions do not blow up for  $h, k \neq 0$  at a fixed time  $t$ ) if the grid spacings  $h, k$  are chosen such that

$$\Delta t / \Delta z = \Delta t / \Delta x = h/k < \left[ \rho(A) + \rho(C) \right]^{-1/2} \quad (16)$$

holds, where  $\rho(A), \rho(C)$  denote the spectral radii of A and C respectively (this is proven rigorously in reference [4]). Then the scheme (13) is first order accurate in time and second order accurate in space.

Artificial boundaries have to be introduced in the sagittal plane in order to obtain a finite-dimensional linear system of equations from (13) and from the discrete boundary conditions at the surface for each time step. The obvious way to do this is to solve (13) in a rectangle (which includes all fingers) and to impose zero Neumann or Dirichlet boundary conditions at those boundaries of the rectangle which do not coincide with the surface. This approach, however, leads to reflections as soon as a wave hits the artificial boundary and therefore has to be abandoned.

Our approach is as follows. At first we split the sagittal plane into subdomains as shown in Figure 1.

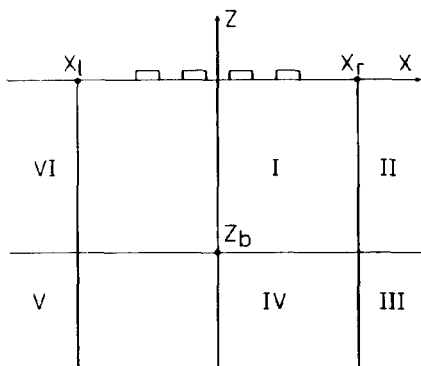


Figure 1

The surface boundary of the rectangle I contains all fingers. Then the unbounded subdomains II-VI are transformed into finite domains and the (transformed) differential equations (13) are discretised in these (finite) auxiliary domains. For example, we make

the following change of variables for the region III:

$$x_3 = 1 - X_r/x, \quad z_3 = -1 + Z_b/z$$

Thus III is mapped into the square  $[0,1] \times [-1,0]$ . The (transformed) differential equations are connected by the requirement that  $u, w, \psi$  are continuous across the boundaries of the subdomains.  $u, w, \psi$  are assumed to vanish in  $x = \pm\infty, z = -\infty$ . Note that  $x = \pm\infty, z = -\infty$  correspond to welldefined lines in the transformed region. This matching gives discrete boundary conditions for the difference scheme (15) on the free boundaries of the rectangle I. No reflections occur since the problem is discretized "on the whole sagittal plane". So this approach gives fully absorbing boundary conditions even when the grids in the transformed auxiliary domains are very coarse. Thus a linear system of equations (of approximate dimension  $3 \cdot (|Z_b|/k) \cdot (|X_l| + |X_r|)/h$ ) has to be solved at each time step. For this we use a so called "Line SOR" iterative method similarly to that used in the computer program package LINPACK [2].

The main advantage of the described difference method compared to the frequently used Fourier transform method is that the difference method can easily be applied to nonlinear elasticity laws while the Fourier method strictly relies on the linearity of the problem.

#### 4. Results

We performed a transient analysis of a four finger transducer structure for two different materials namely YZ-LiNbO<sub>3</sub> and Quartz (ST-cut). The geometry data for both materials are equal such that a fair comparison is possible. The distance between two neighbouring electrodes as well as the finger width amounts 250  $\mu$ m. As described in the previous chapter we observe merely the sagittal plane. The applied voltage on the electrodes is a sinusoidal function in time with a horizontal tangent at  $t=0$  to get consistent initial values. After a quarter period the voltage is a sine function with an amplitude of 0.5 V. As we are mostly interested in surface waves we take the corresponding resonance frequency for both materials namely 3.5 MHz for LiNbO<sub>3</sub> and 3.2 MHz for Quartz.

Figure 2 shows the mechanical displacement  $w$  (with aspect to the "computational" coordinate  $z$  which is the Y-direction of the unrotated crystal

system) for  $\text{LiNbO}_3$  after  $7/4$  periods in a quasi three-dimensional plot. The rectangular bottom of the drawing is the sagittal plane (see Fig. 1) whereas the third dimension represents the dependent variable. One can clearly see that the maximum displacement is on the surface and that the surface wave just leaves the boundary.

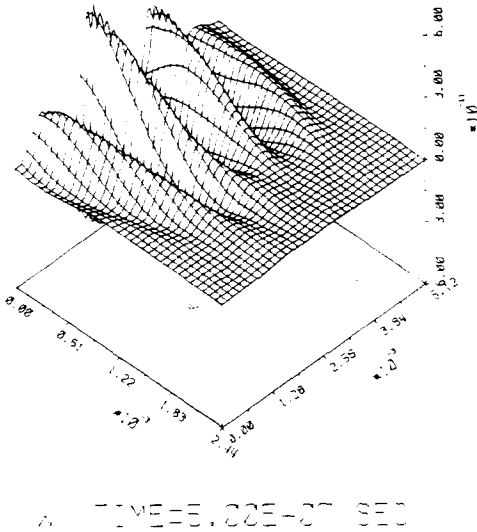


Figure 2

Figure 3 shows a distortion plot of Quartz after two periods. The left vertical boundary represents the surface. The wave amplitude decays fast in the depth of the material. The displacement is much smaller compared to  $\text{LiNbO}_3$ , as the piezoelectric coupling is small (note the unit vector on the right boundary of the figure). The plot clearly demonstrates that the surface wave consists of a transversal as well as a longitudinal component.

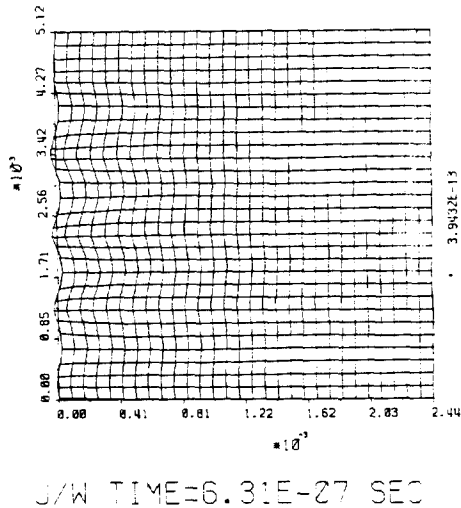


Figure 3

Figure 4 shows the electric potential distribution corresponding to Fig. 3. The unit is Volts (pay attention to the scaling factor on the right boundary). At this time the applied voltage on all electrodes is zero so that this plot represents the mechanical-electrical reaction. One can see that the surface wave passes the boundary without reflection and that the volume wave generation may not be neglected.

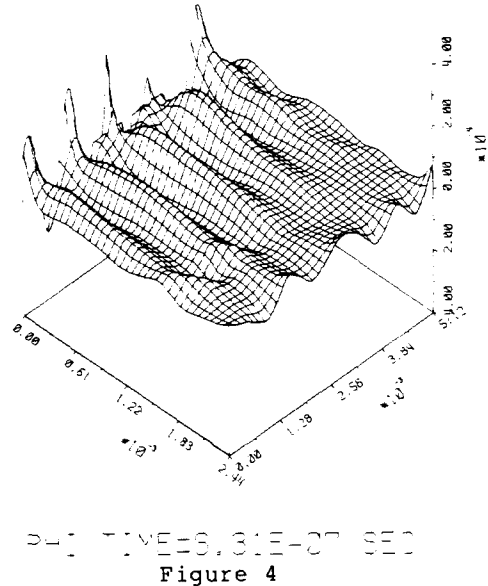


Figure 4

#### References

- [1] Auld B., A.; "Acoustic Fields and Waves in Solids", Wiley, New York, 1973.
- [2] Dongarra J., J. et al.; "LINPACK User's Guide", 1979.
- [3] Kagawa Y. and Yamabuchi T.; Trans. Sonics and Ultrasonics, Vol.SU-23, pp.263, 1976.
- [4] Langer E., Selberherr S., Markowich P., A., Ringhofer Ch., A.; "A Numerical Analysis of a Coupled Elliptic-Hyperbolic Boundary Value Problem Modelling Wave Generation in Piezoelectric Materials", in preparation.
- [5] Milsom R., F., Reilly N., H., C., Redwood M.; Trans. Sonics and Ultrasonics, Vol.SU-24, pp.147, 1977.
- [6] Peach R., C.; Trans. Sonics and Ultrasonics, Vol.SU-28, pp.96, 1981.
- [7] Richtmeyer R., D., Morton N., W.; "Difference Method For Initial Value Problems", 2nd Edition, I. Publishers, I. Trans. Pure a. Appl. Math., 1967.

This work is supported by the "Fond zur Förderung der wissenschaftlichen Forschung" and by Siemens AG.Munich.